Electronic Supplementary Information

Aqueous-processable polymer binder with strong mechanical and polysulfides-trapping properties for high performance lithium-sulfur battery

Huan Yi,[a,b,1] Tu Lan,[c,d,1] Yu Yang,[b,e,1] Zhiwen Lei,[a] Hongbo Zeng,[c,*] Tian Tang,[d] Chaoyang Wang, [a,*] and Yonghong Deng[b,*]

[a]*Research Institute of Materials Science, South China University of Technology, Guangzhou 510640, China*
[b]*Department of Materials Science & Engineering, Southern University of Science and Technology of China, Shenzhen 518055, China*
[c]*Department of Chemical and Materials Engineering, University of Alberta, Edmonton, AB T6G 1H9, Canada*
[d]*Department of Mechanical Engineering, University of Alberta, Edmonton, AB T6G 1H9, Canada*
[e]*Academy for Advanced Interdisciplinary Studies, South University of Science and Technology of China, Shenzhen, China*
[1]*H. Y., T. L. and Y. Y. contributed equally to this work*
**Corresponding authors. E-mail address: hongbo.zeng@ualberta.ca (H.Z.); zhywang@scut.edu.cn; (C.W.); yhdeng08@163.com (Y. H. Deng)*

Table S1. DFT calculations of the thermodynamic parameters (eV) for the various adsorption reactions of Li-S composites at three different lithiation stages (Li_2S, Li_2S_2, and Li_2S_4) on CCS with the monodentate (CCS-*x*-Li_2S_n) and bidentate (CCS-*xy*-Li_2S_n) coordination. Symbols (*x, y*) represent the adsorption sites on CCS.

Adsorption reactions (eV)	ΔG	ΔH	ΔE	E_{BSSE}	ΔE_{bind}
1. CCS-*x*-Li_2S					
(1.1) CCS + Li_2S →CCS-O^1-Li_2S	-0.6869	-0.8603	-0.9050	0.0698	-0.8351
(1.2) CCS + Li_2S →CCS-N^2-Li_2S	-0.8603	-1.0964	-1.1852	0.0997	-1.0855
(1.3) CCS + Li_2S →CCS-O^3-Li_2S	-0.6119	-0.7671	-0.8274	0.0914	-0.7360
(1.4) CCS + Li_2S →CCS-O^4-Li_2S	-0.7413	-1.012	**-1.0696**	0.0999	**-0.9697**
2. CCS-*x*-Li_2S_2					
(2.1) CCS + Li_2S_2 →CCS-O^1-Li_2S_2	-0.4010	-0.8169	-0.8847	0.0872	-0.7975
(2.2) CCS + Li_2S_2 →CCS-N^2-Li_2S_2	-0.6003	-1.0262	-1.1149	0.1143	-1.0005
(2.3) CCS + Li_2S_2 →CCS-O^3-Li_2S_2	-0.3756	-0.7818	-0.8507	0.1120	-0.7387
(2.4) CCS + Li_2S_2 →CCS-O^4-Li_2S_2	-0.4732	-0.9033	**-0.9641**	0.1167	**-0.8474**
3. CCS-*x*-Li_2S_4					
(3.1) CCS + Li_2S_4 →CCS-O^1-Li_2S_4	-0.3343	-0.6827	-0.7467	0.0982	-0.6485
(3.2) CCS + Li_2S_4 →CCS-N^2-Li_2S_4	-0.4771	-0.8770	**-0.9605**	0.1054	**-0.8551**
(3.3) CCS + Li_2S_4 →CCS-O^3-Li_2S_4	-0.4126	-0.9267	-0.9808	0.1451	-0.8357
(3.4) CCS + Li_2S_4 →CCS-O^4-Li_2S_4	-0.5175	-0.9877	**-1.0442**	0.1132	**-0.9310**
4. CCS-*xy*-Li_2S					
(4.1) CCS + Li_2S →CCS-O^1N^2-Li_2S	-0.6084	-0.9193	-0.9662	0.1188	-0.8474
(4.2) CCS + Li_2S →CCS-N^2O^3-Li_2S	-0.6074	-0.9166	-0.9642	0.1196	-0.8446
(4.3) CCS + Li_2S →CCS-O^3O^4-Li_2S	-0.7734	-1.0873	**-1.1518**	0.1760	**-0.9758**
5. CCS-*xy*-Li_2S_2					
(5.1) CCS + Li_2S_2 →CCS-O^1N^2-Li_2S_2	-0.4659	-0.9747	-1.0434	0.1464	-0.8969
(5.2) CCS + Li_2S_2 →CCS-N^2O^3-Li_2S_2	-0.4348	-0.9657	-1.0344	0.1502	-0.8842
(5.3) CCS + Li_2S_2 →CCS-O^3O^4-Li_2S_2	-0.6849	-1.2017	**-1.2673**	0.2052	**-1.0621**
6. CCS-*xy*-Li_2S_4					
(6.1) CCS + Li_2S_4 →CCS-O^1N^2-Li_2S_4	-0.5288	-1.0463	-1.1040	0.1295	-0.9745
(6.2) CCS + Li_2S_4 →CCS-N^2O^3-Li_2S_4	-0.2349	-0.7278	-0.8063	0.1418	-0.6644
(6.3) CCS + Li_2S_4 →CCS-O^3O^4-Li_2S_4	-0.4867	-1.0181	**-1.0786**	0.2002	**-0.8784**

All calculations were carried out within the framework of density functional theory (DFT)[1] by using the hybrid B3LYP functional[2,3] as implemented in the Gaussian 09 package.[4] The split-valence-shell Gaussian basis set, 6-31+G(d,p),[5] was employed to handle H, C, N, O, S and Li atoms for full optimization. The term E_{BSSE} is the energy of the basis set superposition error (BSSE) obtained by using the counterpoise method proposed by Boys and Bernardi.[6]

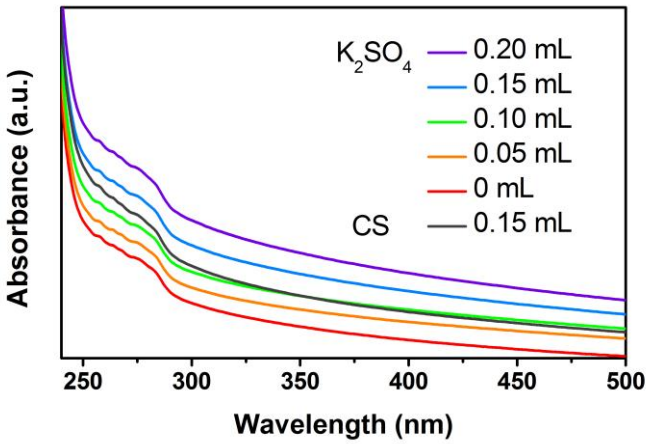

Fig. S1 The determination of sulfate group in CS by gelatin-barium sulfate turbidity.

The gelatin-barium sulfate turbidity experiment for determination on the degree of sulfation was conducted based on the previously described method with minor modification.[7]

Preparation of Gelatin-Barium Chloride solution: 1 g of gelatin was dissolved in 100 mL of DI water at 65 ^{o}C, and the solution was placed at 4 ^{o}C overnight. Then, 0.5 g of barium chloride was added into the solution, and the obtained gelatin-barium chloride solution was standby for next process.

Pretreatment of CCS: 0.1 g of CS was dissolved in a vial with 8 mL of 2M HCl solution, and sealed, kept in 105 ^{o}C to hydrolysis for 4 hours. After that, the vial was cooled down to room temperature. The pH of the solution was adjusted to 6 by ammonium hydroxide, and diluted with water to 25 mL solution.

Measurement of standard curves: 1 mg mL^{-1} of the K_2SO_4 solution was prepared as a standard solution. Then, a K_2SO_4 standard solution of 0, 0.05, 0.1, 0.15, 0.2 mL was added into the cuvette and filled to 200 μL with DI water in all cuvette. After dispersed uniformly, 3.8 mL of 0.2 M HCl, and 1 mL gelatin-barium chloride solution were added in all cuvette respectively. The standard curves were measured by UV-vis after 30 minutes of reaction.

Measurement of CS solution: 0.15 mL of CS solution was added into the cuvette, followed with the addition of 0.05 mL DI water, 3.8 mL of 0.2 M HCl, and 1 mL gelatin-barium chloride solution. After mixed and reacted for 30 minutes, the UV-vis spectrum of the sample was measured, and the absorbance in 360 nm was monitored. The degree of sulfation in CS (η) was calculated by:

$$\frac{0.1}{174}\times 10^{-3} = \frac{0.15\times 0.1}{(161+96\eta)\times 25}\times \eta$$

All experiments were performed in three times to ensure accuracy, and the average value was calculated. The degree of sulfation in CS (η) was calculated to be 16.98%. This data should be slightly lower because of the incomplete hydrolysis of CS during the pretreatment.

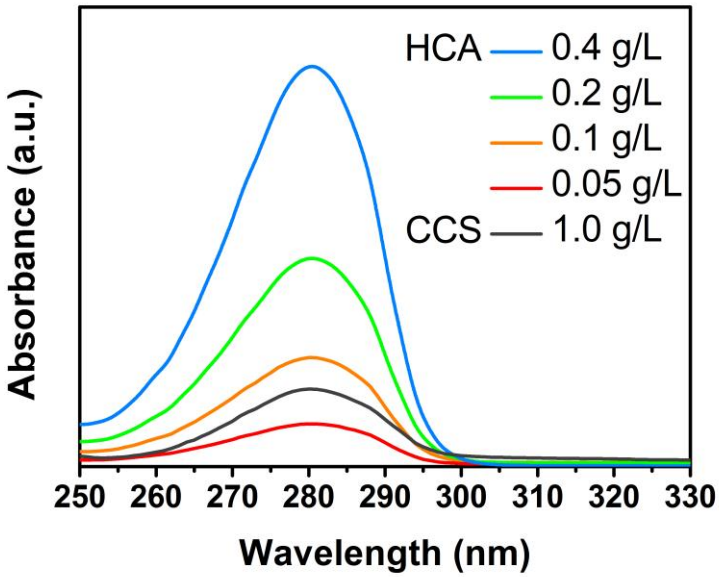

Fig. S2 UV-vis spectra of CCS solution and HCA solution with different concentration.

The degree of catechol conjugation on CCS measured by UV-vis was calculated to be 8.36%. The difference on catechol conjugation results is due to the potential error on deacetylation rate of chitosan.

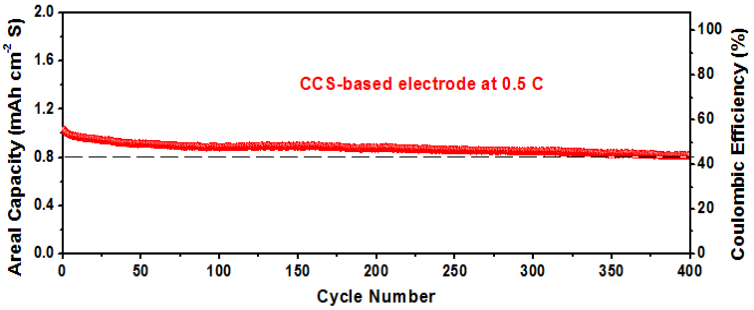

Fig. S3 The areal capacity of CCS-based sulfur electrode at a rate of 0.5 C for 400 cycles.

The areal capacity of the CCS-based sulfur cathode at a rate of 0.5 C for 400 cycles is shown in Fig. R1. The initial areal capacity of the electrode was higher than 1 mAh cm^{-2}, and kept stabilized at about 0.8 mAh cm^{-2} after 400 cyles, indicating the significance of CCS binder in stable cycling performance of sulfur cathode.

Considering that the preparation of this cathode is based on a common sulfur/carbon composite and aluminum foil as current collector, we believe that the areal capacity of CCS-based sulfur cathode can be further elevated by cooperating CCS binder with other advanced technology in lithium sulfur battery, including the carbon matrix of sulfur, separator and electrolyte.

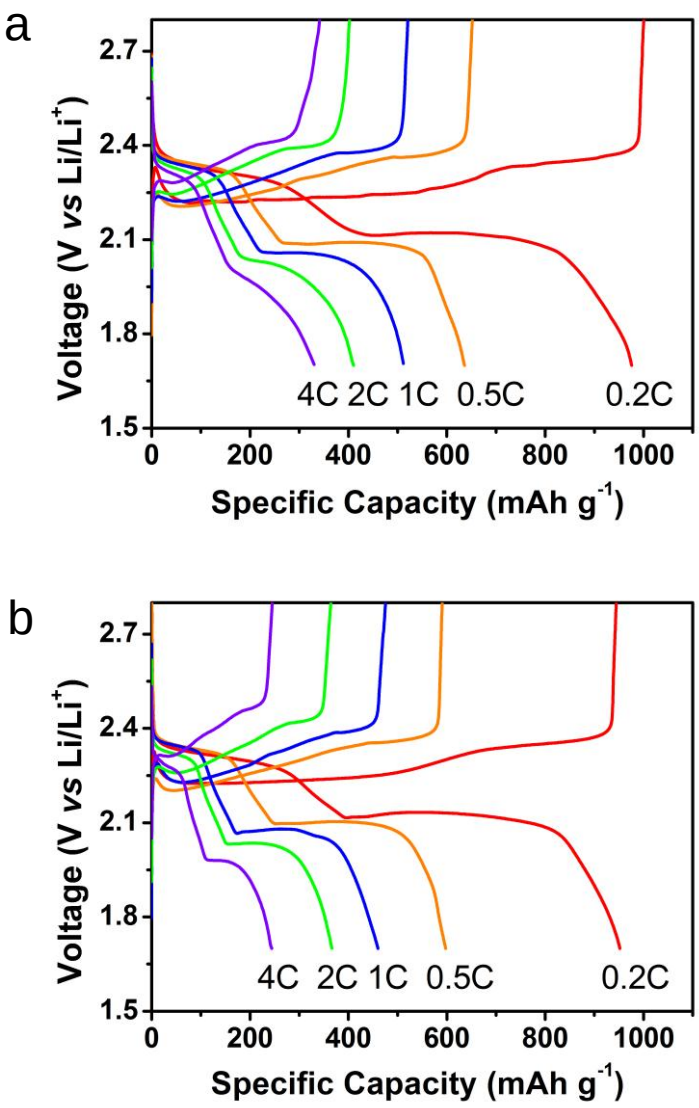

Fig. S4 Charge-discharge profiles of (a) chitosan and (b) PVDF based electrodes from the rate of 0.2 C to 4 C.

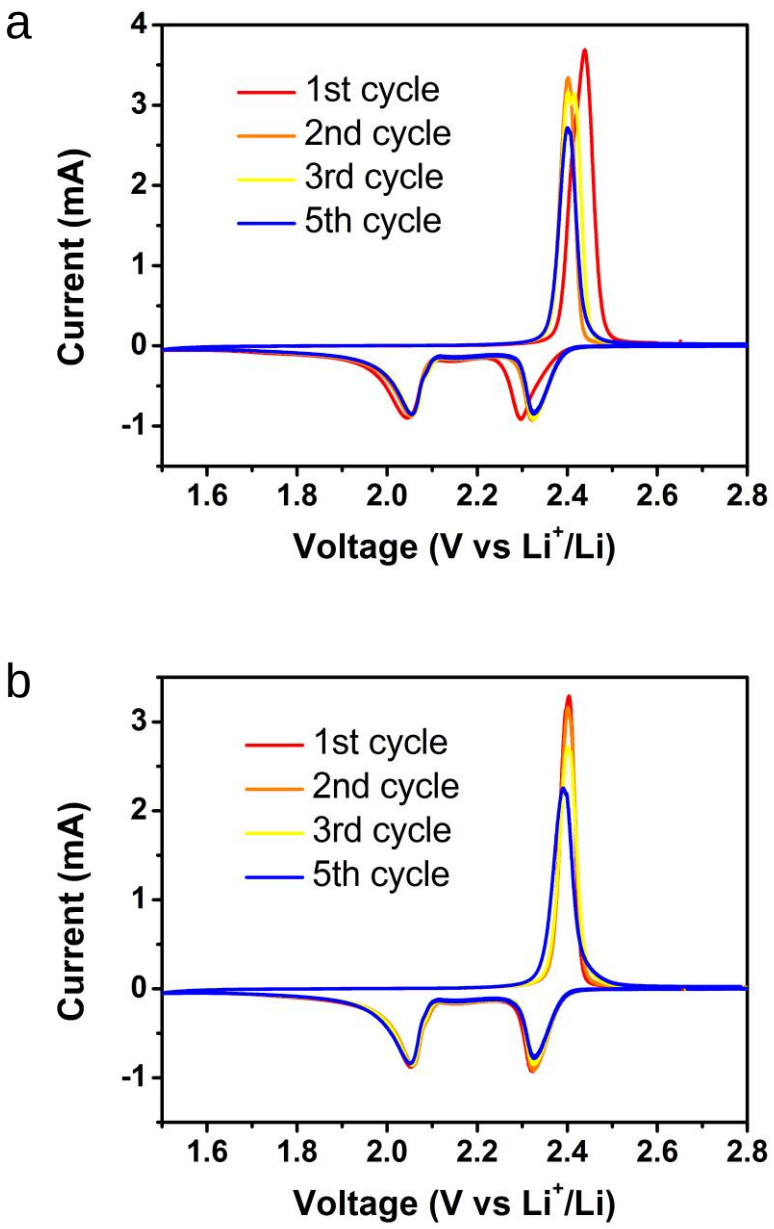

Fig. S5 CV profiles of the (a) chitosan and (b) PVDF based electrodes.

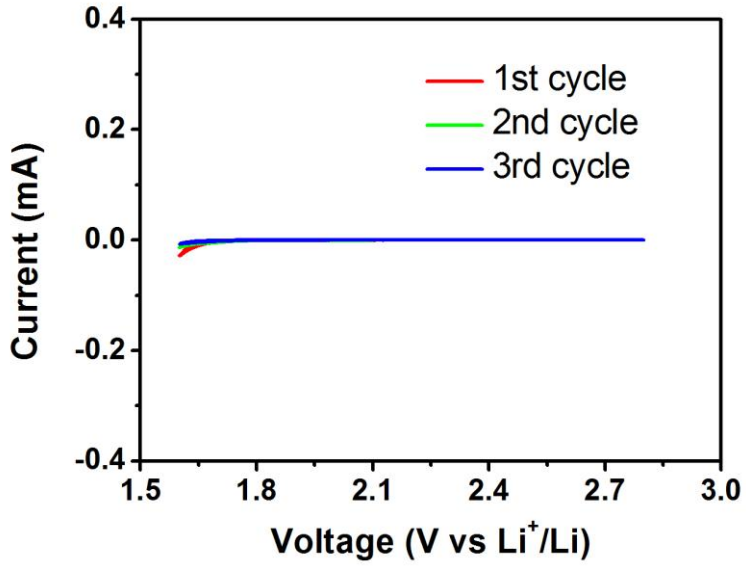

Fig. S6 The CV of electrode with conductive addictive and CCS binder (1:1 in weight).

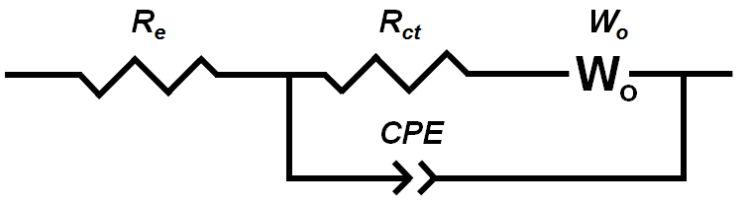

Fig. S7 The equivalent circuit model of the cells in EIS measurement.

In the equivalent circuit model of the cells, R_e represents the resistance of electrolyte, and R_{ct} represents the charge transfer resistance between the interfaces of carbon/sulfur/electrolyte. W_o refers to the Warburg impedance, while CPE refers to the constant phase element. The diameter of the impedance semicircles is related to the charge transfer resistance, which is a measure of the difficulty involved for charges crossing the boundary between the electrode and electrolyte.[8]

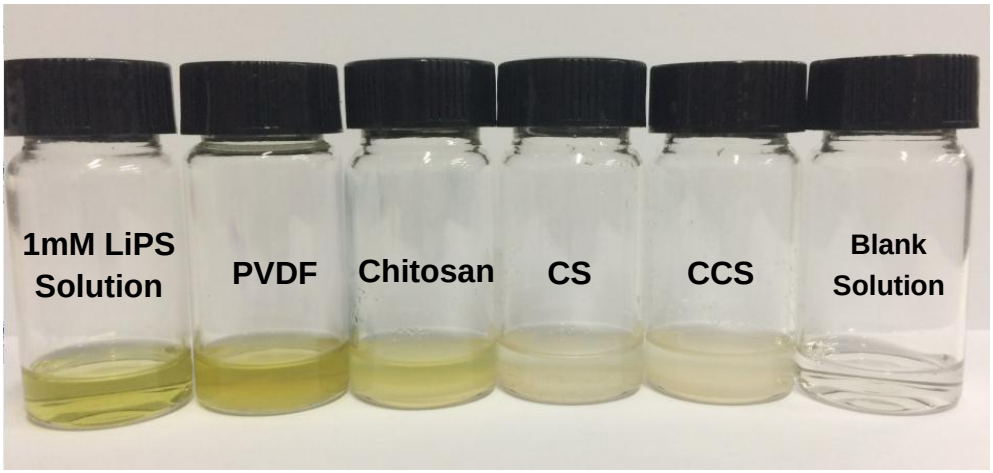

Fig. S8 Optical image of 1mM LiPS solution, blank solution (without LiPS) and solutions after exposed to 0.1 g of PVDF, chitosan, CS, CCS for 5 hours.

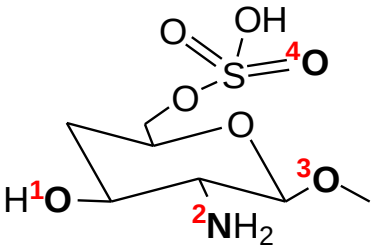

Fig. S9 Schematic elucidation of the model of CCS with four adsorption sites: O^1, N^2, O^3, and O^4.

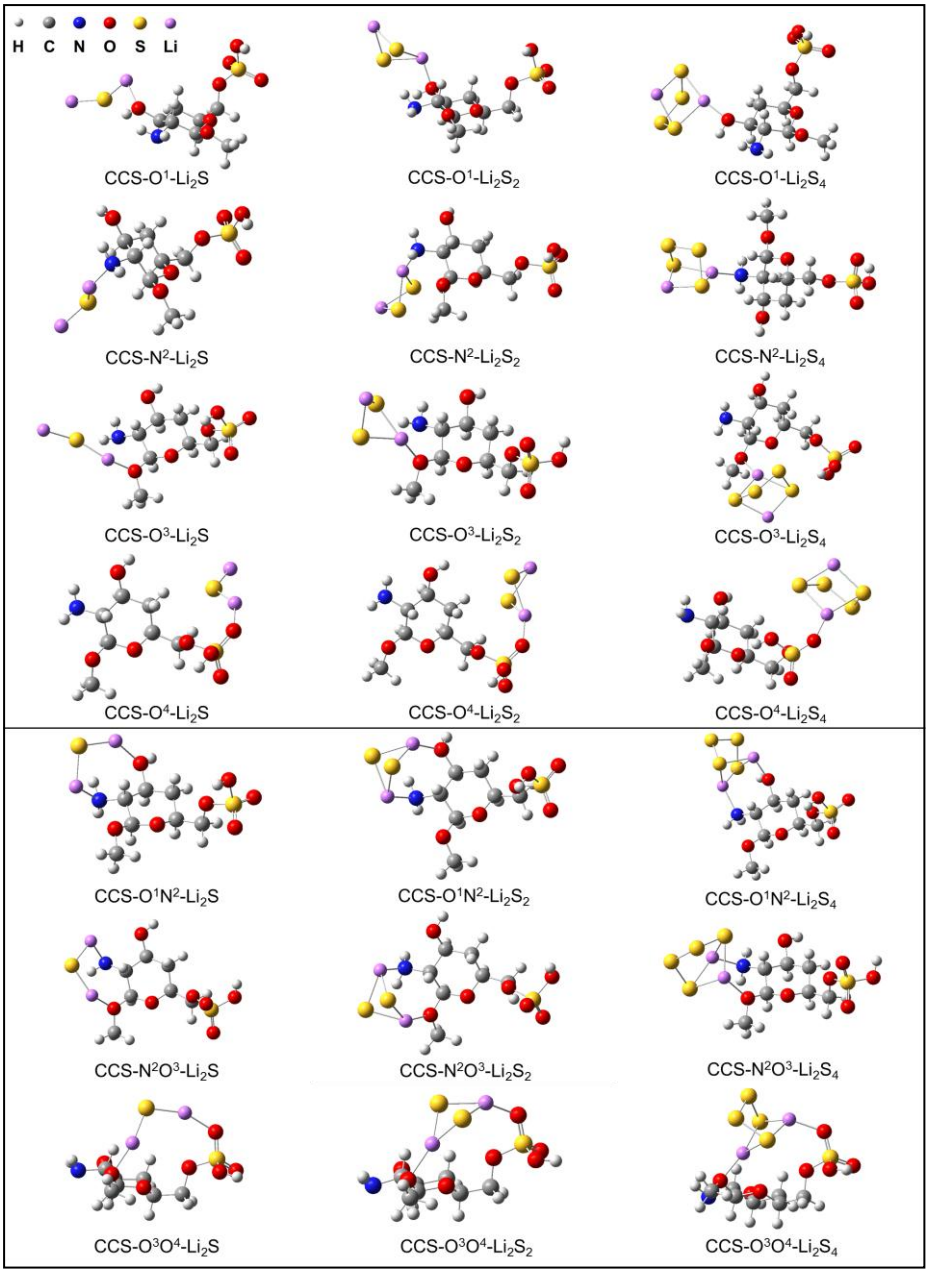

Fig. S10. Fully optimized structures of the stationary points for Li-S composites at three different lithiation stages (Li_2S, Li_2S_2, and Li_2S_4) on CCS. The definition of adsorption sites is shown in Figure S6. The white, gray, blue, red, yellow, and magenta colors represent hydrogen, carbon, nitrogen, oxygen, sulfur, and lithium atoms, respectively. The upper and lower parts displayed the monodentate and bidentate coordination of Li_2S_n on CCS respectively.

Fig. S11 Optical image of the setup, and schematic of the sample for the peeling test.

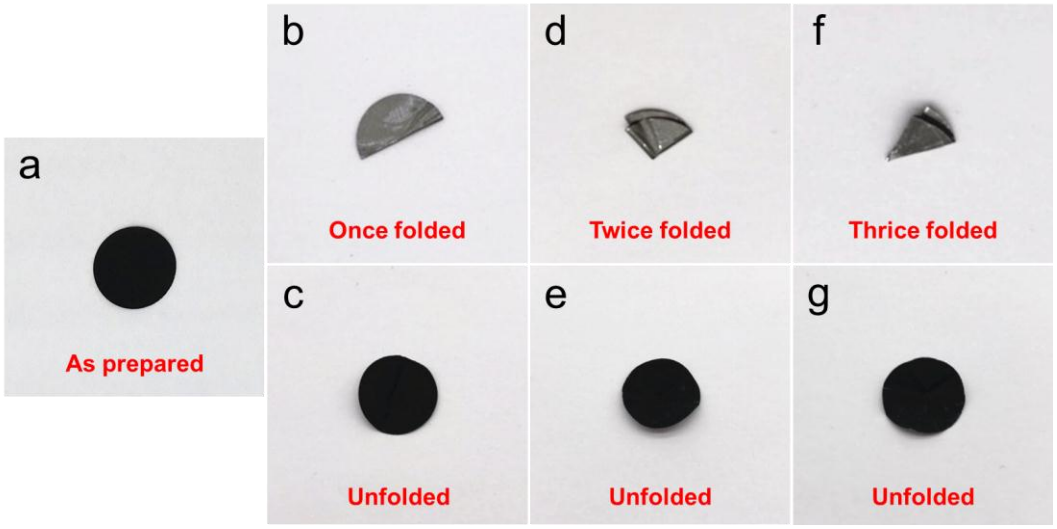

Fig. S12 The digital photographs of (a) the as prepared CCS-based electrode, and (b-g) the electrode after being once, twice and thrice folded, and their corresponding unfolded states

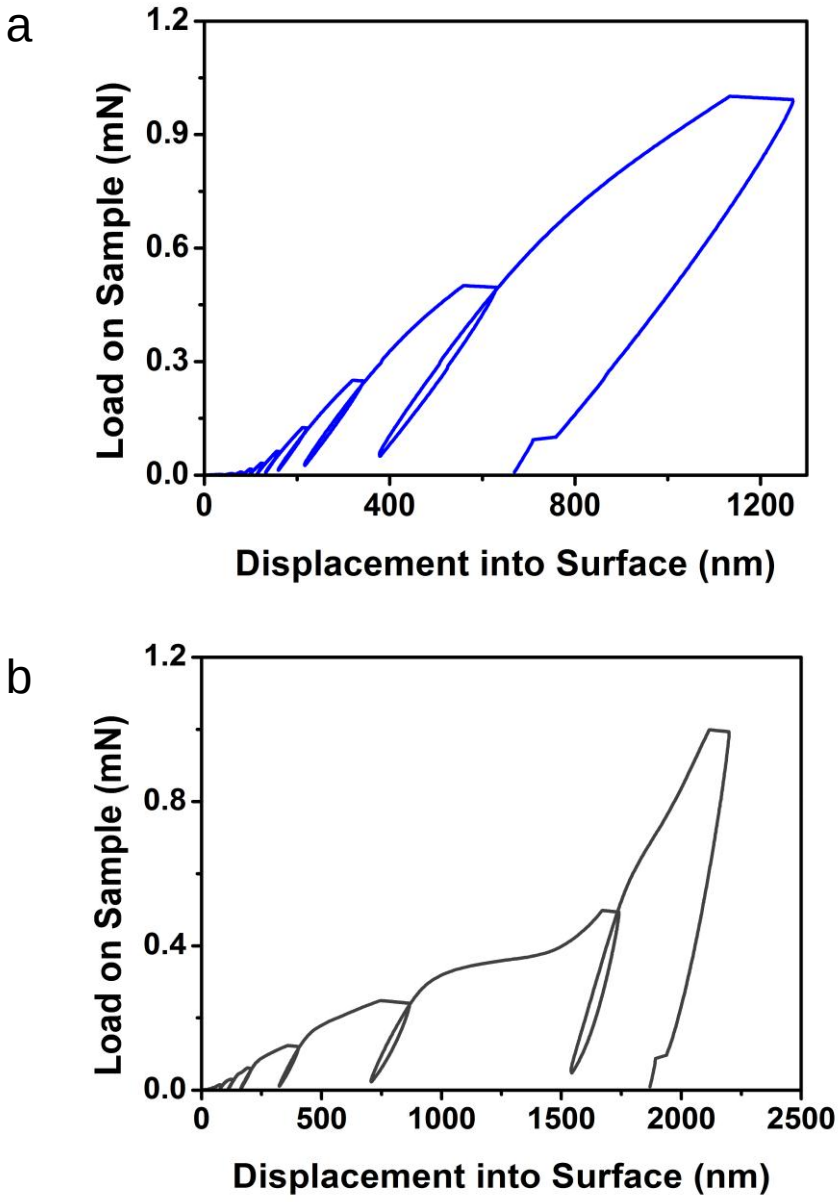

Fig. S13 Typical load−indentation depth curve of (a) chitosan and (b) PVDF based electrode obtained from nanoindentation tests.

Nano-indentation tests on electrodes were performed with a load on the sample reached 1 mN. A partial unload function was adopted in the tests to obtain the variation of reduced modulus (E_r) and hardness (H). E_r was the combined modulus of indenter and specimen, and was calculated to be:

$$\frac{1}{E_r} = \frac{(1-v^2)}{E} + \frac{(1-v'^2)}{E'}$$

Here, E and v represent Young's modulus and Poisson's ratio of the specimen respectively, E' and v' are Young's modulus and Poisson's ratio of the indenter respectively. Nine indentations were

conducted at different locations on each sample to confirm the result.

Hardness H is evaluated through the mean contact pressure at full load,

$$H = \frac{P_{\max}}{A}$$

Here, A is the projected area of contact (as distinct from the actual curved area of contact), P_{max} is the maximum load (1 mN in this case).[9]

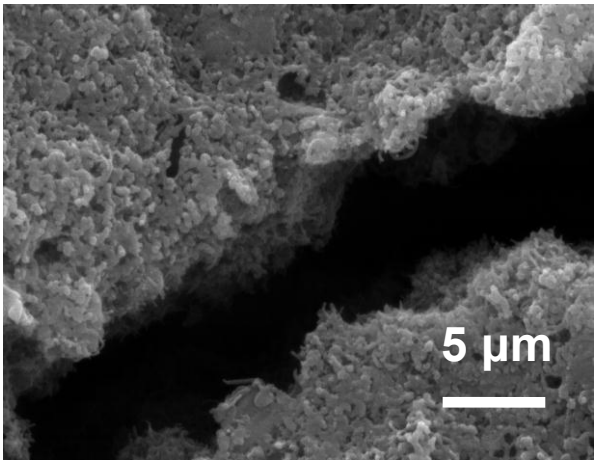

Fig. S14 SEM image of detailed morphology of chitosan-based electrode after 400 cycles at 0.5 C.

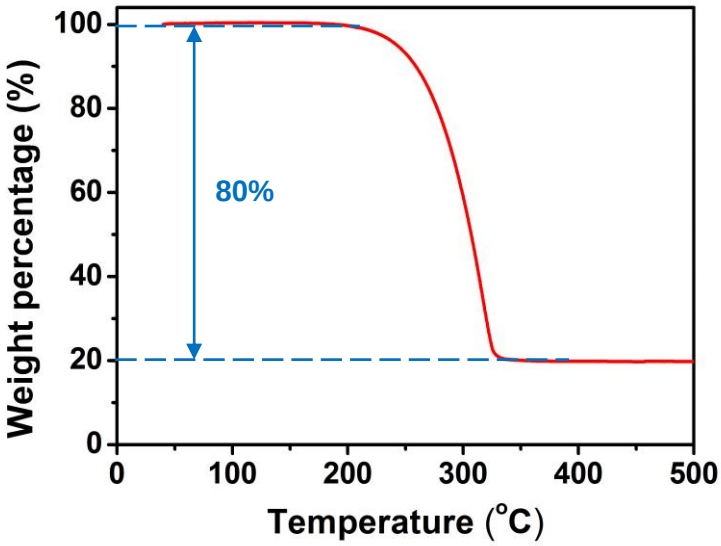

Fig. S15 TGA curve of sulfur/super P composite.

References:

1. Parr, R. G.; Yang, W., *Density Functional Theory of Atoms and Molecules*. Oxford University Press: New York, **1989**.

2. Becke, A. D. Density-functional thermochemistry. III. The role of exact exchange. *J. Chem. Phys.* **1993,** *98*, 5648-5652.

3. Stephens, P. J.; Devlin, F. J.; Chabalowski, C. F.; Frisch, M. J. Ab initio calculation of vibrational absorption and circular dichroism spectra using density functional force fields. *J. Phys. Chem.* **1994,** *98*, 11623-11627.

4. Frisch, M. J.; Trucks, G. W.; Schlegel, H. B.; Scuseria, G. E.; Robb, M. A.; Cheeseman, J. R.; Scalmani, G.; Barone, V.; Mennucci, B.; Petersson, G. A.; Nakatsuji, H.; Caricato, M.; Li, X.; Hratchian, H. P.; Lzmaylov, A. F.; Bloino, J.; Zheng, G.; Sonnenberg, J. L.; Hada, M.; Ehara, M.; Toyota, K.; Fukuda, R.; Hasegawa, J.; Ishida, M.; Nakajima, T.; Honda, Y.; Kitao, O.; Nakai, H.; Vreven, T.; Montgomery, J. A., Jr.; Peralta, J. E.; Ogliaro, F.; Bearpark, M.; Heyd, J. J.; Brothers, E.; Kudin, K. N.; Staroverov, V. N.; Kobayashi, R.; Normand, J.; Raghavachari, K.; Rendell, A.; Burant, J. C.; Lyengar, S. S.; Tomasi, J.; Cossi, M.; Rega, N.; Millam, J. M.; Klene, M.; Knox, J. E.; Cross, J. B.; Bakken, V.; Adamo, C.; Jaramillo, J.; Gomperts, R.; Stratmann, R. E.; Yazyev, O.; Austin, A. J.; Cammi, R.; Pomelli, C.; Ochterski, J. W.; Martin, R. L.; Morokuma, K.; Zakrzewski, V. G.; Voth, G. A.; Salvador, P.; Dannenberg, J. J.; Dapprich, S.; Daniels, A. D.; Farkas, O.; Foresman, J. B.; Ortiz, J. V.; Cioslowski, J.; Fox, D. J. *Gaussian 09*, Gaussian, Inc.: Wallingford, CT, USA, **2009**.

5. Hariharan, P. C.; Pople, J. A. The influence of polarization functions on molecular orbital hydrogenation energies. *Theor. Chim. Acta* **1973,** *28*, 213-222.

6. Boys, S. F.; Bernardi, F. The calculation of small molecular interactions by the differences of separate total energies. Some procedures with reduced errors. *Mol. Phys.* **1970,** *19*, 553-566.

7. Zhu, W.; Ooi, V. E.; Chan , P. K.; Ang, P. O. Isolation and characterization of a sulfated polysaccharide from the brown alga Sargassum patens and determination of its anti-herpes activity. *Biochem. & Cell Biol.* **2003,** 81, 25-33.

8. Su, Y.; Manthiram, A. A facile in situ sulfur deposition route to obtain carbon-wrapped sulfur composite cathodes for lithium–sulfur batteries. *Electrochimica Acta* **2012,** 77, 272-27.

9. Oliver, W. C.; Pharr, G. M. An improved technique for determining hardness and elastic modulus using load and displacement sensing indentation experiments. *J. Mater. Res.* **2011, 7**, 1564-1583.